

Nonlinear Seebeck effect of SU(N) Kondo impurityD. B. Karki^{1,2} and Mikhail N. Kiselev²¹*International School for Advanced Studies (SISSA), Via Bonomea 265, 34136 Trieste, Italy*²*The Abdus Salam International Centre for Theoretical Physics (ICTP) Strada Costiera 11, I-34151 Trieste, Italy* (Received 1 August 2019; revised manuscript received 5 September 2019; published 17 September 2019)

We develop a theoretical framework to study the influence of coupling asymmetry on the thermoelectrics of a strongly coupled SU(N) Kondo impurity based on a local Fermi liquid theory. Applying a nonequilibrium Keldysh formalism, we investigate a charge current driven by the voltage bias and temperature gradient in the strong coupling regime of an asymmetrically coupled SU(N) quantum impurity. The thermoelectric characterizations are made via nonlinear Seebeck effects. We demonstrate that the beyond particle-hole (PH) symmetric SU(N) Kondo variants are highly desirable with respect to the corresponding PH-symmetric setups in order to have significantly improved thermoelectric performance. The greatly enhanced Seebeck coefficients by tailoring the coupling asymmetry of beyond PH-symmetric SU(N) Kondo effects are explored. Apart from presenting the analytical expressions of asymmetry-dependent transport coefficients for general SU(N) Kondo effects, we make a close connection of our findings with the experimentally studied SU(2) and SU(4) Kondo effects in quantum dot nanostructures. Seebeck effects associated with the theoretically proposed SU(3) Kondo effects are discussed in detail.

DOI: [10.1103/PhysRevB.100.125426](https://doi.org/10.1103/PhysRevB.100.125426)**I. INTRODUCTION**

The increasing demand of quantum technologies for energy harvesting has attracted growing attention towards the necessity for nanomaterial-based energy converters [1]. The presence of quantization effects in nanoscale systems allows the controllable comprehension and subsequent control of underlying transport processes [2]. In addition, nanoscale systems can offer greatly enhanced thermoelectric response with respect to conventional bulk counterparts [1–3]. These properties of nanoscale systems have rekindled the field of thermoelectricity [4]. Over the past years, several experiments have resulted in exciting thermoelectric measurements for nanoscale systems, such as quantum dots (QDs), carbon nanotubes (CNTs), quantum point contacts (QPCs), etc. [4–6]. The rapid progress of nanotechnology has allowed the fine-tuning of nanoscale transport process; nonetheless, complete understanding of electron interactions on such a small scale remains the most challenging task [7].

A generic nanodevice consists of a quantum impurity with intrinsic spin S which is tunnel coupled to two electron reservoirs, the source and the drain. The low-energy transport processes are then controlled by the strong interaction between localized spin S and itinerant electrons in the reservoirs. The spin $S = 1/2$ impurity interacting with a single orbital channel of conduction electrons forms a fully screened ground state resulting in quasiparticle resonances at the Fermi level. This paradigmatic screening phenomenon is termed the Kondo effect [8], which is characterized by a low-energy scale T_K , the Kondo temperature. The many-body Kondo resonance at the Fermi level opens an effective path towards the enhancement of thermoelectric production at the nanoscale level [9]. Recent experiments [10–15] have further expanded the scope of transport measurements in Kondo-correlated nanoscale systems. Most of these studies

have been focused on the transport measurement for the spin $S = 1/2$ Kondo impurity described by the SU(2) symmetry group. However, the conventional SU(2) Kondo effects, being protected by particle-hole (PH) symmetry, offer vanishingly small thermoelectric conversion [7]. To achieve appreciable thermopower, the occupation factor of the quantum impurity should be integer, while the PH symmetry should be lifted [16]. The SU(N) Kondo model with integer occupancy m offers the possibility of avoiding a half-filled regime so as to achieve the enhanced thermoelectric production over the conventional SU(2) Kondo-correlated systems [16–18].

The orbital degeneracy of the quantum impurity combines with the true spin symmetry to form the Kondo effect described by higher symmetry group SU(N). Here the occupancy factor m takes all possible values starting from 1 to $N-1$. The paradigmatic SU(4) Kondo physics has been experimentally studied in CNTs [12,19–23], double QDs [24], and single-atom transistors [25]. Various theoretical works [26–31] have contributed towards better understanding of SU(4) Kondo physics over the past years. In addition, exciting proposals have been put forth for the experimental realization of different variants of SU(N) Kondo systems. Possible realization of SU(3) Kondo effects using triple QDs with three- and four-edge states of the quantum Hall effects was suggested in Ref. [32], which been verified recently using a numerical renormalization group study [33]. The proposals for the solid-state realization of SU(6) [34] and SU(12) [35] Kondo effects have likewise attracted considerable attentions both theoretically and experimentally. Beside obtaining the solid-state realization of these exotic SU(N) Kondo effects, an increasing effort has been put into their cold atomic realization [36–39].

Most of the previous studies on SU(N) Kondo effects have been focused solely on charge current measurements.

However, thermoelectric characterization in a generic nanodevice usually involves the Seebeck effects. To the best of our knowledge very few studies have tried to uncover the thermoelectric measurements of Kondo effects described by higher symmetry group. The Seebeck effects with a $SU(4)$ Kondo effect have been studied in Ref. [17], and a general theoretical framework for thermoelectric transport of a $SU(N)$ Kondo model has been developed recently in Ref. [16]. These studies are limited to the setup with perfectly symmetrical tunnel coupling, which is very rarely the case of an experiment. In fact, junction asymmetry could provide important information about the underlying many-body effects [40] and, thus, has to be taken into account in any calculation to compare its result with the experimental data [41]. Therefore unveiling the effects associated with the coupling asymmetry towards the thermoelectric characterization, the Seebeck effects, of a $SU(N)$ Kondo effect has remained a challenging problem for many years. In this contribution we develop a theoretical framework based on a local Fermi-liquid theory in combination with the out-of-equilibrium Keldysh approach to study the influence of coupling asymmetry on the thermoelectric transport of a strongly coupled $SU(N)$ Kondo impurity.

The paper is organized as follows. In Sec. II we discuss in detail the formulation of the model, for thermoelectric transport calculations at the strong-coupling regime of $SU(N)$ Kondo effects, capturing the effects of coupling asymmetry and arbitrary temperature and chemical potentials of the electron reservoirs. We outline the charge current calculations for a $SU(N)$ Kondo impurity which account for both elastic and inelastic effects using the nonequilibrium Keldysh formalism in Sec. III. Section IV is devoted to the summary of our results for the thermoelectric transport coefficients of $SU(N)$ Kondo-correlated systems characterizing the nonlinear Seebeck effects. In this section, apart from presenting the analytical expressions of coupling asymmetry-dependent transport coefficients for general $SU(N)$ Kondo effects, we make a separate analysis of thermoelectrics with (1) experimentally studied $SU(2)$ and $SU(4)$ Kondo effects and (2) theoretically proposed $SU(3)$ Kondo effects. Section V contains the conclusion of our work together with possible future research plans based on the present work.

II. MODEL DESCRIPTION

We consider a quantum impurity tunnel coupled to two conducting reservoirs as shown in Fig. 1. The impurity possesses N -fold degeneracy by combining the spin and other degrees of freedom, such as the orbital degeneracy. In addition, there are N species (orbitals) of electrons in both the left (L) and right (R) reservoirs. The rotation of the reservoir's electrons is then described by the $SU(N)$ transformation. Therefore, to describe our system we start from the $SU(N)$ impurity Anderson model [42,43],

$$H = \sum_{k,r} \varepsilon_k [c_{L,kr}^\dagger c_{L,kr} + c_{R,kr}^\dagger c_{R,kr}] + H_{\text{imp}} + H_{\text{tun}}. \quad (1)$$

Here we introduce the notation “r” to represent the orbital index that takes all possible values starting from 1 to N . The operator $c_{\gamma,kr}^\dagger$ creates an electron with momentum k in the rth

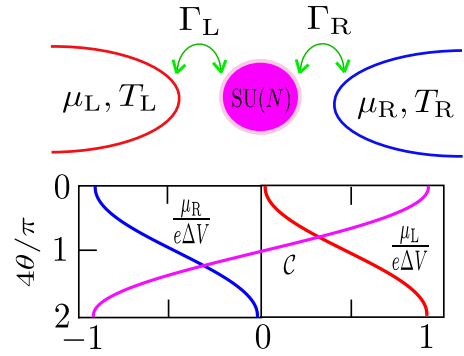


FIG. 1. Upper panel: Schematic representation of an experimental setup for investigating Seebeck effect in nanostructures, where a $SU(N)$ quantum impurity is sandwiched between two conducting reservoirs. The left (red) and right (blue) reservoirs are in thermal equilibrium, separately, at temperature T_L and T_R , respectively. The tunneling-matrix elements from the impurity to the left and right reservoirs are characterized by $t_L = t \cos \theta$ and $t_R = t \sin \theta$ with $\theta \in (0, \pi/2)$. Lower panel: The asymmetry of the tunneling junction is accounted for by introducing a parameter $\mathcal{C} \equiv (\Gamma_L - \Gamma_R)/(\Gamma_L + \Gamma_R) = \cos 2\theta$ with $\Gamma_{L/R} = \pi \rho_{\text{res}} |t_{L/R}|^2$, ρ_{res} being the density of states of the reservoirs. The magenta line represents the variation of asymmetry parameter \mathcal{C} with respect to the asymmetry angle θ . We choose the Fermi level in such a way that the chemical potentials of the left and right reservoirs take some specific values $\mu_{L/R} = \pm \frac{e\Delta V}{2} (1 \mp \mathcal{C})$. This choice of chemical potentials amounts to greatly simplifying the calculation of the charge and heat current through a strongly coupled Kondo impurity (see text for details). These chemical potentials are represented by the red and blue curves, respectively.

orbital of the γ ($= L, R$) reservoir. The energy of conduction electrons ε_k is measured with respect to the chemical potential μ . The second term of Eq. (1) represents the Hamiltonian of the impurity possessing N degenerate flavors with a single energy level ε_d . Then we write the impurity Hamiltonian as

$$H_{\text{imp}} = \varepsilon_d \sum_{\mathbf{r}} d_{\mathbf{r}}^\dagger d_{\mathbf{r}} + U \sum_{\mathbf{r} < \mathbf{r}'} d_{\mathbf{r}}^\dagger d_{\mathbf{r}} d_{\mathbf{r}'}^\dagger d_{\mathbf{r}'}, \quad (2)$$

where $d_{\mathbf{r}}^\dagger$ is the electron creation operator of the impurity and U represents the charging energy, which is assumed to be the largest energy scale of the model. The tunneling processes from the impurity to the reservoirs are accounted for by the very last term of Eq. (1),

$$H_{\text{tun}} = \sum_{k,r} (t_L c_{L,kr}^\dagger + t_R c_{R,kr}^\dagger) d_{\mathbf{r}} + \text{H.c.} \quad (3)$$

We explicitly assume the tunneling asymmetry by assigning the tunneling-matrix elements t_γ such that $t_L = t \cos \theta$ and $t_R = t \sin \theta$ with $\theta \in (0, \pi/2)$. Then the intrinsic total local level width associated with the tunneling is given by $\Gamma_\gamma = \pi \rho_{\text{res}} |t_\gamma|^2$ with ρ_{res} being the density of states of the reservoirs. For the sake of clarity, we introduce the parameter $\mathcal{C} \equiv (\Gamma_L - \Gamma_R)/(\Gamma_L + \Gamma_R) = \cos 2\theta$ to characterize the asymmetry of the tunneling junction. This asymmetry further appears in the Glazman-Raikh rotation [44] of Eq. (1) in the basis of

reservoir's electrons

$$\begin{pmatrix} b_{kr} \\ a_{kr} \end{pmatrix} = \begin{pmatrix} \cos \theta & \sin \theta \\ \sin \theta & -\cos \theta \end{pmatrix} \begin{pmatrix} c_{L,kr} \\ c_{R,kr} \end{pmatrix}. \quad (4)$$

Note that the transformation (4) effectively decouples the operators a_{kr} from the impurity degrees of freedom. Here we consider the general case of having an arbitrary number of electrons $m = 1, 2, \dots, N-1$ in the impurity. Therefore, the specific choice of impurity level $\varepsilon_d = U(1-m-m/N)$ provides the fundamental representation with $\sum_r d_r^\dagger d_r \equiv \sum_r n_r = m$. We then perform the Schrieffer-Wolff transformation [45] followed by the rotation (4) of the Hamiltonian (1) to project out the charge states, which results in

$$\mathcal{H} = \sum_{k,r} \varepsilon_k (a_{kr}^\dagger a_{kr} + b_{kr}^\dagger b_{kr}) + H_{\text{Kondo}}. \quad (5)$$

The Kondo Hamiltonian is expressed in terms of antiferromagnetic coupling J_K between the impurity spin \vec{S} and the spin operator of reservoir electrons placed at the origin \vec{T} as [40,46,47]

$$H_{\text{Kondo}} = J_K \vec{S} \cdot \vec{T}, \quad J_K = \frac{t^2}{U} \frac{N^2}{m(N-m)}. \quad (6)$$

The N^2-1 traceless components of impurity spin $S^i (i = 1, 2, \dots, N^2-1)$ are given by $S^{r,r'} = d_r^\dagger d_{r'} - m/N \delta_{r,r'}$ with the constraint $r, r' \neq N, N'$. Likewise, the spin operator of reservoir electrons placed at the origin is expressed as $\vec{T} = \sum_{kk',r,r'} b_{kr}^\dagger \Lambda_{rr'}^i b_{k'r'}$, Λ^i being the $N \times N$ generators of SU(N) group. Note that S^i are $\frac{N!}{m!(N-m)!} \times \frac{N!}{m!(N-m)!}$ matrices acting on states with m electrons.

The ground state of the spin $S = 1/2$ SU(N) impurity considered in this work is characterized by the complete screening of the impurity spin, which results in the formation of the Kondo singlet. The low-energy regime of the fully screened Kondo effect is consistently described by FL theory [48–50]. Applying the standard point-splitting procedure [16,40,47,49] to the Hamiltonian (6) imparts the low-energy FL Hamiltonian of the SU(N) Kondo impurity,

$$\begin{aligned} \mathcal{H}_0 &= v \sum_r \int_\varepsilon \varepsilon [a_{\varepsilon r}^\dagger a_{\varepsilon r} + b_{\varepsilon r}^\dagger b_{\varepsilon r}], \\ \mathcal{H}_{\text{el}} &= - \sum_r \int_{\varepsilon_{1-2}} \left[\frac{\alpha_1}{2\pi} (\varepsilon_1 + \varepsilon_2) + \frac{\alpha_2}{4\pi} (\varepsilon_1 + \varepsilon_2)^2 \right] b_{\varepsilon_1 r}^\dagger b_{\varepsilon_2 r}, \quad (7) \\ \mathcal{H}_{\text{int}} &= \sum_{r < r'} \int_{\varepsilon_{1-4}} \left[\frac{\phi_1}{\pi v} + \frac{\phi_2}{4\pi v} \sum_{j=1}^4 \varepsilon_j \right] : b_{\varepsilon_1 r}^\dagger b_{\varepsilon_2 r} b_{\varepsilon_3 r'}^\dagger b_{\varepsilon_4 r'} :. \end{aligned}$$

The PH-symmetric version of Eq. (7) was originally proposed by Nozieres [48] and is commonly known as Nozieres FL theory. In Eq. (7) the density of states per species for a one-dimensional channel is represented by the symbol v . The scattering (elastic) effects in the FL are accounted for by the Hamiltonian \mathcal{H}_{el} , where α_1 and α_2 are the first and second generations of Nozieres FL coefficients, respectively. The four fermions term represents the interaction part of the Hamiltonian \mathcal{H}_{int} , which is expressed in terms of FL parameters ϕ_1 and ϕ_2 . These FL parameters are related to the associated Kondo temperature of the corresponding SU(N) impurity.

The FL parameters characterizing the scattering effects are connected to those of the interaction effects by the relation $\alpha_1 = (N-1)\phi_1$ and $\alpha_2 = (N-1)\phi_2/4$. In addition the Bethe ansatz provides a further link between α_1 and α_2 [40,47],

$$\mathcal{A} \equiv \frac{\alpha_2}{\alpha_1^2} = \frac{N-2}{N-1} \frac{\Gamma(1/N) \tan(\pi/N)}{\sqrt{\pi} \Gamma(\frac{1}{2} + \frac{1}{N})} \cot \left[\frac{m\pi}{N} \right], \quad (8)$$

where $\Gamma(x)$ is the Euler's gamma function. Therefore the low-energy FL Hamiltonian (7) is completely specified by only one FL parameter, say, α_1 . We make a connection of α_1 with the corresponding Kondo temperature such that $T_K^{\text{SU}(N)} = 1/\alpha_1$, and the N dependence in FL parameters is implicit. Note that we have retained up to the four fermions term in Eq. (7); the higher-order terms produce the current correction beyond cubic order in the applied bias and temperature gradient, which is beyond the scope of present work.

It is then a straightforward procedure to proceed with the calculation of physical observables by treating the scattering Hamiltonian \mathcal{H}_{el} and interaction part \mathcal{H}_{int} perturbatively. However, in the spirit of Nozieres phenomenology, the scattering effects are fully described by an energy-dependent phase shift $\delta_r^{\text{el}}(\varepsilon)$. The Kondo singlet acts as the scatterer for the incoming electrons from the leads. Outgoing and incoming electrons then differ from each other by the elastic phase shift $\delta_r^{\text{el}}(\varepsilon)$. The Nozieres FL parameters α_1 and α_2 are the first- and second-order coefficients in the Taylor-series expansion of the elastic phase shift. While the scattering effects are easily accounted for by the elastic phase shift, the perturbative treatment of \mathcal{H}_{int} produces complicated self-energy diagrams. This complication can be simplified a bit by including the Hartree contribution of self-energy in the elastic phase shift [40,47]. Then the Taylor expansion of the phase shift reads

$$\begin{aligned} \delta_r(\varepsilon) &= \delta_0 + \alpha_1 \varepsilon + \alpha_2 \varepsilon^2 - \sum_{r' \neq r} \left\{ \phi_1 \int_{-\infty}^{\infty} d\varepsilon \delta n_{r'}(\varepsilon) \right. \\ &\quad \left. + \frac{\phi_2}{2} \left[\varepsilon \int_{-\infty}^{\infty} d\varepsilon \delta n_{r'}(\varepsilon) + \int_{-\infty}^{\infty} d\varepsilon \varepsilon \delta n_{r'}(\varepsilon) \right] \right\}. \quad (9) \end{aligned}$$

Here the zero-energy phase shift of the SU(N) Kondo impurity with m electrons is

$$\delta_0 = \frac{m\pi}{N}. \quad (10)$$

In Eq. (9) we used the definition of the actual FL quasiparticle distribution relative to the Fermi energy ε_F as $\delta n_r(\varepsilon) \equiv n_r(\varepsilon) - \Theta(\varepsilon_F - \varepsilon) = \langle b_{kr}^\dagger b_{kr} \rangle - \Theta(\varepsilon_F - \varepsilon)$, Θ being the step function. Using Eq. (4) we expressed the average $\langle b_{kr}^\dagger b_{kr} \rangle$ in terms of the equilibrium Fermi-distribution functions $f_{\gamma}(\varepsilon) = [1 + \exp(\frac{\varepsilon - \mu_{\gamma}}{T})]^{-1}$ of the left and right reservoirs, and $\langle b_{kr}^\dagger b_{kr} \rangle = \cos^2 \theta f_L + \sin^2 \theta f_R$. In addition, we have implemented the specific choice of Fermi level such that

$$\int_{-\infty}^{\infty} d\varepsilon \delta n_r(\varepsilon) = 0. \quad (11)$$

This equation is always satisfied as far as the condition $\mu_L \cos^2 \theta + \mu_R \sin^2 \theta = \varepsilon_F$ is fulfilled. We then made the

following specification for the chemical potentials of the reservoirs:

$$\mu_L = e\Delta V \sin^2 \theta \equiv \frac{e\Delta V}{2}(1 - C), \quad (12)$$

$$\mu_R = -e\Delta V \cos^2 \theta \equiv -\frac{e\Delta V}{2}(1 + C), \quad (13)$$

to make $\varepsilon_F = 0$. It is also noted that the details related to the choice of the temperatures in the reservoirs do not affect the necessary condition to satisfy Eq. (11). To be more general, we do not yet impose any restriction on the choice of T_L and T_R . Using these specifications of chemical potentials and temperatures of the reservoirs, the straightforward integration of the phase shift expression (9) leads to

$$\delta_r(\varepsilon) = \delta_0 + \alpha_1 \varepsilon + \alpha_2 (\varepsilon^2 - \mathcal{A}). \quad (14)$$

To obtain Eq. (14) we have made the use of FL identity $\alpha_2 = (N-1)\phi_2/4$ and the new definition,

$$\mathcal{A} = \frac{1}{6} \left[(\pi T_L)^2 (1+C) + (\pi T_R)^2 (1-C) + \frac{3}{2} (1-C^2) (e\Delta V)^2 \right].$$

In the following section the scattering effects in addition to the Hartree contribution to the self-energy correction will be accounted for by Eq. (14). To obtain the self-energy correction beyond the Hartree contribution we will be treating the interaction Hamiltonian $\mathcal{H}_{int}^{\text{SU}(N)}$ perturbatively with the small parameters $(e\Delta V, T_L, T_R)/T_K^{\text{SU}(N)}$.

III. CURRENT CALCULATION

The nonlinear Seebeck coefficient, the central object of this work, directly follows from the solution of the zero charge current condition (see Sec. IV). The charge current in the $\text{SU}(N)$ Kondo regime consists of two parts: the elastic and inelastic. While the elastic effects are accounted for by the scattering phase shift, inelastic corrections have to be treated perturbatively as illustrated earlier. Therefore, to proceed further with the calculation, one needs to have an expression of an operator representing the charge current. Though there exist several possible ways of writing the charge current [40], we use the the basis of scattering states that includes the elastic effects and Hartree term to write the charge current operator in the form [40,51]

$$\hat{I} = \frac{e}{2h\nu} \sum_r \sin 2\theta [a_r^\dagger(x) b_r(x) - a_r^\dagger(-x) \mathcal{E} b_r(-x) + \text{H.c.}], \quad (15)$$

for $b_r(x) = \sum_k b_{kr} e^{ikx}$ and $\mathcal{E} b_r(x) = \sum_k \mathcal{E}_k b_{kr} e^{ikx}$. To write Eq. (15) we have also omitted the terms of the form $\sum_{r,p=\pm} p a_r^\dagger(px) a_r(px)$ since they do not produce a finite contribution to the mean current. In addition, we expressed the $N \times N$ scattering matrix \mathcal{E}_k in terms of the phase shift expression (14) such that $\mathcal{E}_k = \exp[2i\delta_r(\varepsilon_k)]$. To compute the various observables from Eq. (15) we need the following averages directly obtained from the Glazman-Raikh rotation:

$$\begin{pmatrix} \langle b_k^\dagger b_k \rangle \\ \langle a_k^\dagger a_k \rangle \\ \langle b_k^\dagger a_k \rangle \end{pmatrix} = \begin{pmatrix} \cos^2 \theta & \sin^2 \theta & 0 \\ \sin^2 \theta & \cos^2 \theta & 0 \\ \frac{\sin 2\theta}{2} & -\frac{\sin 2\theta}{2} & 0 \end{pmatrix} \begin{pmatrix} f_L(\varepsilon_k) \\ f_R(\varepsilon_k) \\ 0 \end{pmatrix}. \quad (16)$$

The average of Eq. (15) provides the elastic current (including the corresponding Hartree contribution), which has the compact form analogous to the Landauer-Büttiker expression

$$I_{el} = \frac{e}{h} \sum_r \int_{-\infty}^{\infty} d\varepsilon \mathcal{T}_r(\varepsilon) [f_L(\varepsilon) - f_R(\varepsilon)]. \quad (17)$$

The effective transmission coefficient $\mathcal{T}_r(\varepsilon)$ is completely specified by the phase shift expression (14); $\mathcal{T}_r(\varepsilon) \equiv (1 - C^2) \sin^2[\delta_r(\varepsilon)]$. To write $\mathcal{T}_r(\varepsilon)$ into a more tractable form, we perform its Taylor expansion in energy and retain up to the second-order terms,

$$\mathcal{T}_r(\varepsilon) = (1 - C^2) [\mathcal{T}_0 - \alpha_2 \mathcal{A} \sin 2\delta_0 + \alpha_1 \sin 2\delta_0 \varepsilon + (\alpha_1^2 \cos 2\delta_0 + \alpha_2 \sin 2\delta_0) \varepsilon^2]. \quad (18)$$

Here $\mathcal{T}_0 = \sin^2 \delta_0$ is the zero energy transmission coefficient. Then it is a trivial procedure to compute the elastic current by plugging Eq. (18) into Eq. (17). The exact computation of Eq. (17) follows from the consideration of the following integrals [51,52]:

$$\mathcal{K}_n = \int_{-\infty}^{\infty} \varepsilon^n [f_L(\varepsilon) - f_R(\varepsilon)] d\varepsilon, \quad n = 0, 1, \text{ and } 2. \quad (19)$$

The conventional way of calculating the integrals in Eq. (19) consists of Sommerfeld expansion of $\Delta f(\varepsilon) \equiv f_L(\varepsilon) - f_R(\varepsilon)$ in the small parameters $\Delta T \equiv T_L - T_R$ and ΔV . However, the Fourier-transform technique allows us to compute Eq. (19) exactly. Fourier transforming the function $\Delta f(\varepsilon)$ into real time reads

$$\Delta f(t) = \frac{1}{2\pi} \int_{-\infty}^{\infty} d\varepsilon e^{-i\varepsilon t} \Delta f(\varepsilon). \quad (20)$$

Performing the n -times partial differentiation of Eq. (20) and taking the limit $t \rightarrow 0$ we get

$$\frac{2\pi}{(-i)^n} \left. \frac{\partial^n \Delta f(t)}{\partial t^n} \right|_{t=0} = \int_{-\infty}^{\infty} d\varepsilon \varepsilon^n \Delta f(\varepsilon). \quad (21)$$

Fourier transformation of the Fermi distributions of the left and right reservoirs allows us to write

$$\Delta f(t) = \frac{i}{2} \left[\frac{T_L e^{-i\mu_L t}}{\sinh(\pi T_L t)} - \frac{T_R e^{-i\mu_R t}}{\sinh(\pi T_R t)} \right]. \quad (22)$$

Plugging Eq. (22) into Eq. (21) with the chemical potentials as specified in Eqs. (12) and (13), we obtain $\mathcal{K}_0 = e\Delta V$, $\mathcal{K}_1 = [(\pi T_L)^2 - (\pi T_R)^2 - 3C(e\Delta V)^2]/6$, and

$$\mathcal{K}_2 = \frac{e\Delta V}{3} \left[\frac{(e\Delta V)^2}{4} (1 + 3C^2) + \frac{1-C}{2} (\pi T_L)^2 + \frac{1+C}{2} (\pi T_R)^2 \right].$$

For completeness we reexpress the elastic current in terms of the integrals in Eq. (19) as

$$I_{el} = \frac{Ne(1 - C^2)}{h} [(\mathcal{T}_0 - \alpha_2 \mathcal{A} \sin 2\delta_0) \mathcal{K}_0 + \alpha_1 \sin 2\delta_0 \mathcal{K}_1 + (\alpha_1^2 \cos 2\delta_0 + \alpha_2 \sin 2\delta_0) \mathcal{K}_2]. \quad (23)$$

Now we turn to the discussion of inelastic effects leaving aside the Hartree contributions, which has been already accounted for by the phase shift expressed in Eq. (14). As we anticipated earlier, the perturbative treatment of \mathcal{H}_{int} imparts the interaction corrections to the charge current. This approach requires the expressions of noninteraction Green's functions (GFs) described by \mathcal{H}_0 . The matrices of the noninteracting GFs in Keldysh space [53] are given by

$$\mathcal{G}_{bb/aa}(k, \varepsilon) = \frac{1}{\varepsilon - \varepsilon_k} \tau_z + i\pi \begin{pmatrix} F_{b/a} & F_{b/a+1} \\ F_{b/a-1} & F_{b/a} \end{pmatrix} \delta(\varepsilon - \varepsilon_k),$$

$$\mathcal{G}_{ba/ab}(k, \varepsilon) = i\pi \begin{pmatrix} 1 & 1 \\ 1 & 1 \end{pmatrix} F_{ab} \delta(\varepsilon - \varepsilon_k). \quad (24)$$

Here the parameters $F_{b/a}(\varepsilon)$ and $F_{ab}(\varepsilon_k)$ are expressed in terms of different populations; $F_b(\varepsilon_k) = 2\langle b_k^\dagger b_k \rangle - 1$, $F_a(\varepsilon_k) = 2\langle a_k^\dagger a_k \rangle - 1$ and $F_{ab} = 2\langle b_k^\dagger a_k \rangle$. The z -component of the Pauli matrix is represented by τ_z . However, in the flat-band limit only the off-diagonal parts of $\mathcal{G}_{bb}(k, \varepsilon)$, namely, $\mathcal{G}_{bb}^{+-}(k, \varepsilon)$ and $\mathcal{G}_{bb}^{-+}(k, \varepsilon)$, produce the finite contribution to the charge current. The straightforward mathematical steps provide the following Fourier-transformed real-time GFs:

$$\mathcal{G}_{bb}^{+-}(t) = -\frac{\pi\nu}{2} \left[\frac{T_L(1+C)e^{-i\mu_L t}}{\sinh(\pi T_L t)} + \frac{T_R(1-C)e^{-i\mu_R t}}{\sinh(\pi T_R t)} \right],$$

$$\mathcal{G}_{ab/ba}(t) = -\frac{\pi\nu}{2} \sqrt{1-C^2} \left[\frac{T_L e^{-i\mu_L t}}{\sinh(\pi T_L t)} - \frac{T_R e^{-i\mu_R t}}{\sinh(\pi T_R t)} \right]. \quad (25)$$

Here $\mathcal{G}_{bb}^{+-}(t)$ and $\mathcal{G}_{bb}^{-+}(t)$ are connected by causality relations. In practice, the GFs expressed in Eqs. (24) and (25) are sufficient for the calculation of the charge current. To calculate the inelastic correction to the charge current we then apply the perturbation theory using the Keldysh formalism [53],

$$\delta I_{\text{in}} = \langle T_C \hat{I}(t) e^{-i \int dt' \mathcal{H}_{\text{int}}(t')} \rangle, \quad (26)$$

where C denotes the double-sided $\eta = \pm$ Keldysh contour and T_C is corresponding time-ordering operator. We used the expression of the charge current operator (15) and interaction Hamiltonian \mathcal{H}_{int} into Eq. (26) to obtain the interaction correction to the charge current

$$\delta I_{\text{in}} = \mathcal{L} \int_{-\infty}^{\infty} \frac{d\varepsilon}{2\pi} (\Sigma^{-+} - \Sigma^{+-})(\varepsilon) i\pi\nu \Delta f(\varepsilon). \quad (27)$$

To arrive from Eq. (26) to Eq. (27) we have already subtracted the diverging terms, which amounts to the renormalization of FL coefficients (see Ref. [40] for details). In addition, we introduced the new notation via $\mathcal{L} = \frac{N(N-1)}{h} e\pi(1-C^2) \cos 2\delta_0$. The self-energies in Eq. (27) are expressed in real time as

$$\Sigma^{\eta_1\eta_2}(t) = \left(\frac{\phi_1}{\pi\nu^2} \right)^2 \sum_{k_1, k_3} [\mathcal{G}_{bb}^{\eta_1\eta_2}(k_1, t) \times \mathcal{G}_{bb}^{\eta_2\eta_1}(k_2, -t) \mathcal{G}_{bb}^{\eta_1\eta_2}(k_3, t)]. \quad (28)$$

For the calculation of self-energies, now we specify the temperatures of the left and right reservoirs $T_R = T$ and $T_L = T + \Delta T$ with $\Delta T > 0$. In practice one can numerically solve for the self-energy using the GFs of Eq. (25). However, it is

manageable to find the analytical expression of the self-energy difference to the first order in ΔT and second order in $e\Delta V$, which reads

$$(\Sigma^{-+} - \Sigma^{+-})(\varepsilon) = \frac{\phi_1^2}{i\pi\nu} \left[\frac{3}{4} (e\Delta V)^2 (1 - C^2) + \varepsilon^2 + (\pi T)^2 + \frac{\Delta T}{T} (\pi T)^2 (1 + C) \right]. \quad (29)$$

To arrive from Eq. (28) to Eq. (29) we came across the integral of the form

$$\mathcal{Z}(a, T) = \int_{-\infty}^{\infty} \frac{e^{iat}}{\sinh^3(\pi T t)} dt. \quad (30)$$

The singularity of the integral in Eq. (30) is removed by shifting the time contour by $i\eta$, $\eta \rightarrow 0$ in the complex plane. The parameter η is chosen such that $\eta D \gg 1$ and $(\eta T, \eta \Delta T, \eta \Delta V) \ll 1$ with D the band cutoff. We chose the rectangular contour enclosing the singularity at $t = 0$ and use Cauchy's residue theorem to arrive at the result

$$\mathcal{Z}(a, T) = -i\pi \frac{a^2 + (\pi T)^2}{(\pi T)^2} \frac{1}{\exp(a/T) + 1}. \quad (31)$$

Equation (29) contains all possible terms up to the linear response in ΔT and ΔV . Therefore plugging Eq. (29) into Eq. (27) provides an interaction correction up to the quadratic order in ΔT and ΔV . To make interaction contributions to the charge current more symmetrical with that of elastic effects, we write

$$\delta I_{\text{in}} = \frac{Ne(1-C^2)}{h} \frac{1}{2} \frac{1}{N-1} \cos 2\delta_0 \alpha_1^2 \times \left\{ \mathcal{K}_2 + \left[\frac{\Delta T}{T} (\pi T)^2 (1 + C) + (\pi T)^2 \right] \mathcal{K}_0 \right\}. \quad (32)$$

This equation correctly reproduces the interaction correction up to the quadratic response with the coefficients $\mathcal{K}_{0,2}$ given in Eq. (19). Using Eqs. (23) and (32), the charge current is given by

$$I_c = I_{\text{el}} + \delta I_{\text{int}}. \quad (33)$$

IV. RESULTS AND DISCUSSION

The nonlinear Seebeck effect is quantified by the Seebeck coefficient defined as the ratio of thermovoltage developed under the condition of zero charge current, $\Delta V_{\text{th}} \equiv \Delta V|_{I_c=0}$, to the applied temperature gradient [54,55],

$$S \equiv - \frac{\Delta V_{\text{th}}}{T_L - T_R} \Big|_{I_c=0}. \quad (34)$$

In fact, the Seebeck coefficient Eq. (34) contains additional information than the electrical and thermal conductance measurements [56]. While the electrical conductance depends merely on the density of states at the Fermi level, the Seebeck coefficient reveals its slope [57]. In addition, the Seebeck coefficient provides the useful information related to the average energy of charge carriers contributing to the transport processes [58]. We characterize the Seebeck coefficient of a SU(N) Kondo impurity by defining the dimensionless form

of the charge current accounting for up to the quadratic responses,

$$\begin{aligned} \mathcal{J}(N, m) &\equiv \frac{I_c(N, m)}{G_0(N)T_K^{\text{SU}(N)}} \\ &= \mathcal{L}_1^1 \Delta \bar{V} + \mathcal{L}_2^1 \Delta \bar{T} + \mathcal{L}_1^2 \Delta \bar{V}^2 + \mathcal{L}_2^2 \Delta \bar{T}^2 \\ &\quad + \mathcal{L}_{12}^{11} \Delta \bar{V} \Delta \bar{T}. \end{aligned} \quad (35)$$

The maximum conductance of the SU(N) Kondo impurity in the presence of asymmetry is expressed by the relation $G_0(N) = (1 - \mathcal{C}^2)Ne^2/h$. From now we use the electronic charge $e = -1$ and the convention $\Delta V > 0$ and $\Delta T > 0$. The quantities written in overline letters represent that they are normalized with the corresponding Kondo temperature: $\bar{T} \equiv T/T_K^{\text{SU}(N)}$, $\Delta \bar{T} \equiv \Delta T/T_K^{\text{SU}(N)}$, and $\Delta \bar{V} \equiv \Delta V/T_K^{\text{SU}(N)}$. From Eqs. (23) and (32) we obtained the transport coefficients \mathcal{L}_j^i and \mathcal{L}_{12}^{11} , $i, j = 1, 2$ for the SU(N) Kondo impurity,

$$\begin{aligned} \mathcal{L}_1^1 &= \left[\sin^2 \left(\frac{\pi m}{N} \right) + \frac{1}{3} \frac{N+1}{N-1} \cos \left(\frac{2\pi m}{N} \right) (\pi \bar{T})^2 \right], \\ \mathcal{L}_2^1 &= -\frac{\pi^2}{3} \bar{T} \sin \left(\frac{2\pi m}{N} \right), \quad \mathcal{L}_1^2 = \frac{1}{2} \mathcal{C} \sin \left(\frac{2\pi m}{N} \right), \\ \mathcal{L}_2^2 &= -\frac{\pi^2}{6} \sin \left(\frac{2\pi m}{N} \right), \\ \mathcal{L}_{12}^{11} &= -\frac{\pi^2}{3} \bar{T} \left[\mathcal{B} \cos \left(\frac{2\pi m}{N} \right) + 2\mathcal{C} \mathcal{A} \sin \left(\frac{2\pi m}{N} \right) \right]. \end{aligned} \quad (36)$$

The coefficient \mathcal{A} is defined in Eq. (8), and \mathcal{B} stands for

$$\mathcal{B} \equiv \frac{\mathcal{C}(N-2) - N - 1}{N-1}. \quad (37)$$

Equation (36) shows that the transport coefficients accounting for the linear and quadratic correction in the temperature gradient are connected by the relation $\mathcal{L}_2^1 = 2\bar{T} \mathcal{L}_2^2$. It is apparent that merely the asymmetry of the junction is responsible to have the quadratic correction in the voltage bias. For half-filled SU(N) Kondo effects, we observed that $\mathcal{L}_2^1 = \mathcal{L}_1^2 = \mathcal{L}_2^2 = 0$; therefore, corresponding thermoelectric properties are governed by only two coefficients \mathcal{L}_1^1 and \mathcal{L}_{12}^{11} . This fact explains that the half-filled SU(N) Kondo impurity does not offer finite thermopower even in a quadratic-response level of calculations. Another important conclusion that can be drawn from Eq. (36) is as follows; for the perfectly symmetrical quarter-filled SU(N) Kondo-correlated systems, the combined effects of temperature gradient and voltage bias tend to vanish: $\mathcal{L}_{12}^{11}|_{\mathcal{C}=0}(N, N/4) = 0$. Furthermore, the coefficients characterizing the voltage response do not acquire the temperature correction. These facts should make the nonlinear thermoelectric measurement of beyond half-filled SU(4) systems a trivial procedure. To have more insights into the thermoelectric production in SU(N) Kondo systems, we solve the zero current condition of Eq. (35) to get the thermovoltage up to the quadratic terms in $\Delta \bar{T}$,

$$-\Delta \bar{V}_{\text{th}} = \mathcal{S}^{\text{LR}} \Delta \bar{T} + \delta \mathcal{S} (\Delta \bar{T})^2 + O(\Delta \bar{T})^3. \quad (38)$$

The Seebeck coefficient \mathcal{S} as defined in Eq. (34) then takes the form

$$\mathcal{S} = \mathcal{S}^{\text{LR}} + \delta \mathcal{S} \Delta \bar{T} + O(\Delta \bar{T})^2. \quad (39)$$

Here \mathcal{S}^{LR} is the linear response Seebeck coefficient, and its first-order $\Delta \bar{T}$ correction is defined by $\delta \mathcal{S}$,

$$\mathcal{S}^{\text{LR}} \equiv \frac{\mathcal{L}_2^1}{\mathcal{L}_1^1}, \quad (40)$$

$$\delta \mathcal{S} \equiv \left[\frac{\mathcal{L}_2^2}{\mathcal{L}_1^1} - \frac{\mathcal{L}_2^1 \mathcal{L}_{12}^{11}}{(\mathcal{L}_1^1)^2} + \frac{(\mathcal{L}_2^1)^2 \mathcal{L}_1^2}{(\mathcal{L}_1^1)^3} \right]. \quad (41)$$

The transport coefficients defining the linear response Seebeck coefficient \mathcal{S}^{LR} are independent of asymmetry parameter \mathcal{C} . However, the first-order correction $\delta \mathcal{S}$ bears the strong dependences on the asymmetry parameter via the transport coefficients \mathcal{L}_1^1 and \mathcal{L}_{12}^{11} . In addition, for the symmetrical setups, we use Eq. (36) to express the correction factor $\delta \mathcal{S}$ entirely in terms of linear-response coefficients,

$$\delta \mathcal{S}|_{\mathcal{C}=0} = \frac{\mathcal{S}^{\text{LR}}}{\bar{T}} \left[\frac{\sin^2 \left(\frac{\pi m}{N} \right)}{\mathcal{L}_1^1} - \frac{1}{2} \right]. \quad (42)$$

To study the effects of coupling asymmetry on the thermoelectric transport properties, we categorize the SU(N) Kondo impurity into two broad classes, namely, half-filled (PH-symmetric) and beyond half-filled, and discuss them separately.

A. PH-symmetric SU(N) Kondo effects

The low-energy regime of the SU(N) Kondo effects with the half-filling $m = N/2$ is protected by the emergent PH symmetry; an example includes the conventional SU(2) Kondo effect. In these systems, the zero energy phase shift reaches the unitary value $\delta_0 = \pi/2$ resulting in the maximal conductance. While the PH symmetry is responsible for enhanced electronic properties, the corresponding thermoelectric transport coefficient gets suppressed due to the effect of a highly symmetrical transmission coefficient. As we anticipated earlier that the half-filled Kondo effects satisfy the relation $\mathcal{L}_2^1 = \mathcal{L}_1^2 = \mathcal{L}_2^2 = 0$, therefore, corresponding thermoelectric properties are derived solely from the coefficients \mathcal{L}_1^1 and \mathcal{L}_{12}^{11} . The nonzero transport coefficients of PH-symmetric SU(N) Kondo effects are summarized as

$$\mathcal{L}_1^1(N, N/2) = \left[1 - \frac{1}{3} \frac{N+1}{N-1} (\pi \bar{T})^2 \right], \quad (43)$$

$$\mathcal{L}_{12}^{11}(N, N/2) = \frac{1}{3\bar{T}} \left[\frac{\mathcal{C}(N-2) - N - 1}{N-1} \right] (\pi \bar{T})^2. \quad (44)$$

While for the conventional SU(2) Kondo effects the parameter \mathcal{C} does not affect the cross-coefficient, the corresponding measurement in SU($N > 2$) PH-symmetric systems depends on the coupling asymmetry.

The PH symmetry of the Kondo impurity realized in QDs is exact only if the dot is tuned to the middle of Coulomb valley [59]. This indicates the possibility of breaking the underlying PH symmetry. This weakly broken PH symmetry of Kondo-correlated systems is accounted for by renormalizing the reference phase shifts such that [60–62]

$$\delta_0 \rightarrow \tilde{\delta}_0 = \delta_0 + \delta_p, \quad \delta_0 \gg \delta_p. \quad (45)$$

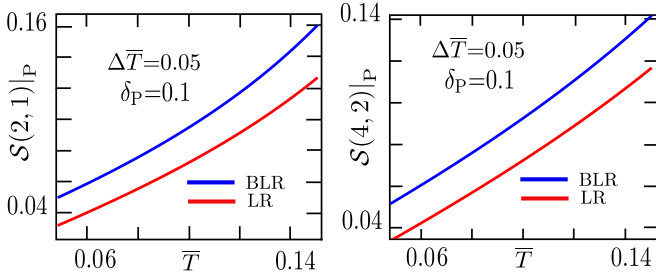


FIG. 2. Linear (LR) and nonlinear (BLR) Seebeck coefficients with PH-symmetric SU(2) and SU(4) Kondo effects for a fixed value of the potential scattering δ_P .

This potential scattering provides the repulsive interactions which breaks the Kondo singlet and contributes to inelastic processes [63]. The first-order transport coefficients in Eq. (36) for PH-symmetric Kondo-correlated systems with an account of the potential scattering effects are then given by

$$\begin{aligned} \mathcal{L}_1^{\mathcal{L}}(N, N/2)|_P &= \cos^2 \delta_P \left[1 - \frac{(\pi \bar{T})^2}{3} \frac{N+1}{N-1} \frac{2 \cos 2\delta_P}{1 + \cos 2\delta_P} \right], \\ \mathcal{L}_2^{\mathcal{L}}(N, N/2)|_P &= \cos^2 \delta_P \left[\frac{(\pi \bar{T})^2}{3\bar{T}} \frac{2 \sin 2\delta_P}{1 + \cos 2\delta_P} \right]. \end{aligned} \quad (46)$$

Equation (46) allows us to compute the linear response Seebeck coefficient of PH-symmetric SU(N) Kondo effects with small potential scattering,

$$\mathcal{S}^{\text{LR}}(N, N/2)|_P = \frac{2}{3} \frac{1}{\bar{T}} \frac{(\pi \bar{T})^2}{1 - \frac{(\pi \bar{T})^2}{3} \frac{N+1}{N-1}} \delta_P + O(\delta_P)^3. \quad (47)$$

Note that due to the numerical factor $(N+1)/(N-1)$ in the denominator of Eq. (47), among PH-symmetric generalizations of SU(N) the SU(2) Kondo-correlated systems offer the highest value of the linear response Seebeck coefficient in the presence of finite potential scattering. Plugging Eq. (45) into the transport coefficients Eq. (36) and using them in Eq. (41), we get the first-order correction to the Seebeck coefficient up to the linear order in δ_P ,

$$\delta \mathcal{S}(N, N/2)|_P = \frac{\pi^2}{3} \frac{1 - \frac{(\pi \bar{T})^2}{3} \left(\frac{N+1}{N-1} + 2\mathcal{B} \right)}{\left[1 - \frac{(\pi \bar{T})^2}{3} \frac{N+1}{N-1} \right]^2} \delta_P + O(\delta_P)^3. \quad (48)$$

For SU(2) Kondo effects the correction (48) is independent of the asymmetry parameter as can be inferred from Eq. (37). However, for SU(4) and other PH-symmetric versions of SU(N), the first-order correction to the Seebeck effect is weakly asymmetry dependent via the coefficient $\mathcal{B}(\mathcal{C})$. The linear and nonlinear Seebeck coefficients with PH-symmetric SU(2) and SU(4) Kondo effects are shown in Fig. 2 with the choice of potential scattering term $\delta_P = 0.1$ and temperature gradient $\Delta \bar{T} = 0.05$. These significant enhancements of BLR Seebeck coefficients with respect to the corresponding LR contribution get further improved at a relatively high reference temperature and large temperature drop across the junction.

B. Beyond half-filled SU(N) Kondo effects

The SU(N) Kondo effect with an arbitrary integer filling factor $m < N$ offers the possibility of avoiding an undesir-

able PH-symmetric regime for the enhanced thermoelectric coefficient. The Kondo physics beyond the half-filled regime $m/N \neq 1/2$ is described by the asymmetric shape of the transmission coefficient, which is highly desirable to achieve huge thermopower production. In general, the Kondo-correlated systems with $N > 2$ provide the realization of paradigmatic PH-asymmetric setups. In particular, the experimentally studied SU(4) Kondo effect consisting of either a single electron or three electrons would, thus, represents an ideal test bed for the study of beyond half-filled Kondo physics. The special case of the SU(3) Kondo effect can fulfill the two filling conditions $m/N = 1/3$ or $2/3$ both away from the PH-symmetric regime. Considering that, we first start from the SU(3) Kondo effects, and this subsection will be devoted to a discussion of the SU(4) Kondo regime.

The SU(3) Kondo effect can occur with either a single electron or two electrons. The physics of the SU(3) Kondo effect with one and two electrons is related with each other by a PH symmetry transformation. Therefore, we discuss the single-electron SU(3) Kondo systems, which will ultimately provide the corresponding information of the two-electron case. For single-electron SU(3) Kondo effects the transport coefficients in Eq. (36) are simplified as

$$\begin{aligned} \mathcal{L}_1^{\mathcal{L}}(3, 1) &= \frac{3}{4} \left[1 - \frac{4}{9} (\pi \bar{T})^2 \right], & \mathcal{L}_2^{\mathcal{L}}(3, 1) &= -\frac{\pi^2 \bar{T}}{2\sqrt{3}}, \\ \mathcal{L}_1^2(3, 1) &= \mathcal{C} \frac{\sqrt{3}}{4}, & \mathcal{L}_2^2(3, 1) &= -\frac{\pi^2}{4\sqrt{3}}, \\ \mathcal{L}_{12}^{11}(3, 1) &= -\frac{\pi^2}{3} \bar{T} \left\{ \frac{\mathcal{C}}{4} \left(1 - 2\sqrt{\frac{3}{\pi}} \frac{\Gamma[1/3]}{\Gamma[5/6]} \right) - 1 \right\}. \end{aligned} \quad (49)$$

Therefore while the cross coefficient $\mathcal{L}_{12}^{11}(3, 1)$ is weakly asymmetry dependent, the coefficient $\mathcal{L}_1^2(3, 1)$ is strongly influenced by \mathcal{C} . Since all the transport coefficients in Eq. (49) are nonzero, one can solve the zero-current equation to get the thermovoltage developed in SU(3) Kondo effects.

The SU(4) Kondo effects can accommodate up to three electrons. While the two-electron case suffers from the PH symmetry, the single- and three-electron SU(4) systems are regarded to have good thermoelectric performance. Furthermore, the single- and three-electron systems are related to each other by the PH symmetry transformation. Therefore we discuss in details about the thermoelectric of single-electron SU(4) Kondo effects. The corresponding transport coefficients are obtained as

$$\begin{aligned} \mathcal{L}_1^{\mathcal{L}}(4, 1) &= \frac{1}{2}, & \mathcal{L}_2^{\mathcal{L}}(4, 1) &= -\frac{\pi^2}{3} \bar{T}, & \mathcal{L}_1^2(4, 1) &= \frac{\mathcal{C}}{2}, \\ \mathcal{L}_2^2(4, 1) &= -\frac{\pi^2}{6}, & \mathcal{L}_{12}^{11}(4, 1) &= -\frac{4\pi^2 \mathcal{C} \bar{T}}{9\sqrt{\pi}} \frac{\Gamma[1/4]}{\Gamma[3/4]}. \end{aligned} \quad (50)$$

The cross coefficient $\mathcal{L}_{12}^{11}(4, 1) \simeq -7.32\mathcal{C}\bar{T}$ is very large as compared to other coefficients for a relatively large asymmetry parameter. In addition the other coefficient $\mathcal{L}_1^2(4, 1)$ is also strongly asymmetry dependent. The presence of these coefficients is solely manifested by the finite asymmetry of the junction. Therefore we argue that measuring this cross coefficient would be useful while identifying the asymmetry

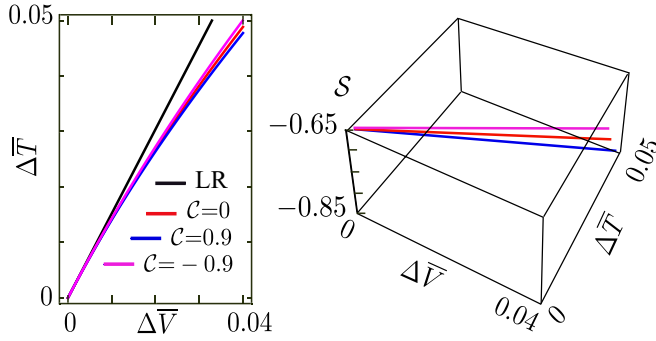


FIG. 3. Left panel: Plot of asymmetry-dependent zero current lines in PH-asymmetric SU(4) Kondo effects within the quadratic response level of calculations as a function of applied voltage bias and temperature gradient at reference temperature $\bar{T} = 0.1$. Right panel: Corresponding Seebeck coefficients for given asymmetry parameter.

of the junction in addition to its physical implications. Just from the structure of Eq. (50), it is seen that the thermoelectric transport properties of beyond half-filled SU(4) Kondo effects can be easily manipulated by tuning the junction asymmetry. It appears that the effect of asymmetry becomes more pronounced in a relatively high-temperature gradient regime. The asymmetry parameter C mainly causes the shift of the zero-current line either upward or downward with respect to the perfectly symmetric setup. As shown in Fig. 3 the positive value of the asymmetry parameter increases the thermovoltage, while the opposite effects are apparent for the corresponding negative values. In addition, the beyond linear response contribution always overshoots the corresponding linear response value irrespective of the coupling asymmetry.

C. Paradigmatic SU(4) Kondo effects

The cosine factor $\cos 2\delta_0$ in front of the expression of the inelastic current dramatically modifies the low-energy transport behavior of SU(N) Kondo effects. In the case of the SU(N) systems with m electrons satisfying the specific combination such that $m/N = (2n + 1)/4$ for $n = 0$ and 1, the cosine factor $\cos 2\delta_0$ in Eq. (32) amounts to nullifying the whole expression. For these specific systems, the beyond Hartree contribution to the self-energy becomes zero, while the corresponding Hartree contribution remains finite. In addition, for PH-symmetric SU(N) Kondo effects the Hartree contribution vanishes and the beyond Hartree contribution becomes finite. Interestingly, the PH-asymmetric SU(4) Kondo-correlated systems offer a vanishing non-Hartree contribution to the self-energy. Since the Hartree contributions can be straightforwardly accounted for by including them in the phase shift, the beyond-half filled SU(4) systems can be exactly solved within cubic response and even beyond. This paradigmatic simplification is also applicable for some SU(12) generalizations. From Eq. (23) we obtained two nonzero cubic response coefficients $\mathcal{L}_1^3(4, 1)$ and $\mathcal{L}_{12}^{12}(4, 1)$ contributing to the charge current of the beyond-half filled SU(4) Kondo impurity as

$$\mathcal{J}(4, 1)|_{\text{cubic}} = \mathcal{L}_1^3(4, 1)(\Delta\bar{V})^3 + \mathcal{L}_{12}^{12}(4, 1)\Delta\bar{V}(\Delta\bar{T})^2.$$

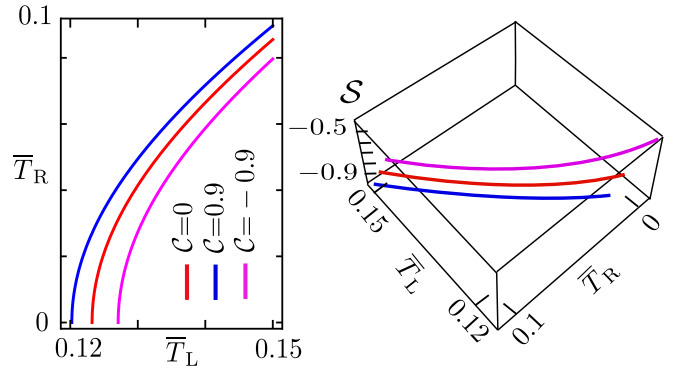


FIG. 4. Left panel: Lines of zero charge currents in a single-electron SU(4) Kondo impurity within the cubic response level of calculations. The temperatures of the left and right reservoirs (normalized with corresponding Kondo temperature) are varied for a given asymmetry parameter at fixed voltage drop $\Delta\bar{V} = 0.05$. Right panel: The Seebeck coefficients as a function of asymmetry parameter with beyond half-filled SU(4) Kondo effects for fixed voltage drop $\Delta\bar{V} = 0.05$.

Here the transport coefficients are

$$\mathcal{L}_1^3(4, 1) = -\frac{1-3C^2}{9\sqrt{\pi}} \frac{\Gamma[1/4]}{\Gamma[3/4]},$$

$$\mathcal{L}_{12}^{12}(4, 1) = -C \frac{2\pi^2}{9\sqrt{\pi}} \frac{\Gamma[1/4]}{\Gamma[3/4]}.$$

These equations show that for the perfectly symmetrical single-electron SU(4) Kondo setups, the effects of voltage bias and temperature gradient are not correlated even in the cubic response level of calculations. Therefore, only the asymmetry can derive these systems to have a combined interplay of voltage bias and temperature gradient. The effects of the asymmetry parameter on the Seebeck coefficient in the cubic response level of calculations are presented in Fig. 4 with an example of single-electron SU(4) Kondo effects. From Fig. 4 it is seen that with the proper choice (positive value) of asymmetry parameter C the nonlinear Seebeck coefficient gets significantly enhanced over the corresponding perfectly symmetrical coupling. This effect is associated with strong asymmetry of the beyond linear response transmission coefficient (18).

Finally we want to mention that the nonlinearly also has been studied by generalizing the definition of the Seebeck coefficient with constant current condition [64–66] such that

$$\bar{S}(N, m) = \frac{\partial \mathcal{J}(N, m)}{\partial \Delta\bar{T}} \bigg/ \frac{\partial \mathcal{J}(N, m)}{\partial \Delta\bar{V}}. \quad (51)$$

In the linear response level of calculation the response coefficient defined in Eq. (51) coincides with the Seebeck coefficient given by Eq. (34). Though their behaviors in the nonlinear regime are quite different, it has been argued that the coefficient \bar{S} is indeed experimentally accessible [64] and can provide an important ingredient for the propose of temperature sensing. These effects already have been studied in the conventional SU(2) Kondo regime accounting for the linear response of temperature gradient and finite voltage bias [64,65]. The central result of the paper expressed in

Eq. (36) paves a straightforward way of extending their study with an account of strong nonlinearity in a more exotic Kondo-correlated system.

V. CONCLUSIONS

We developed a theoretical framework based on a local Fermi-liquid theory in combination with the out-of-equilibrium Keldysh approach to study the influences of coupling asymmetry on the thermoelectric transport of a strongly coupled SU(N) Kondo impurity. While the linear response Seebeck coefficient is independent of coupling asymmetry, the fundamental role of nonlinearity towards the enhancement of the Seebeck coefficient with a SU(N) Kondo setup is explored. In addition, we reported the great enhancement of the Seebeck coefficient of Kondo impurities by properly tailoring the coupling asymmetry. We explored the importance of potential scattering on the thermoelectric characterization of

PH-symmetric SU(N) Kondo effects. The presented analytical expressions of asymmetry-dependent transport coefficients for the general SU(N) Kondo effects allow us to make a close connection of our findings with the experimentally studied SU(2) and SU(4) Kondo effects in complex QD nanostructures. Application of a developed theoretical framework for the investigation of thermoelectric properties of more exotic Kondo problems such as multistage and multiterminal Kondo screening appears to be a valid avenue for future research.

ACKNOWLEDGMENTS

We thank Robert Whitney, Eva Andrei, Yigal Meir, Yuval Oreg, Giulio Casati, and Giuliano Benenti for illuminating discussions. This work was performed in part at Aspen Center for Physics, which is supported by National Science Foundation under Grant No. PHY-1607611. This work was partially supported (M.K.) by a grant from the Simons Foundation.

-
- [1] M. S. Dresselhaus, G. Dresselhaus, X. Sun, Z. Zhang, S. B. Cronin, and T. Koga, *Phys. Solid State* **41**, 679 (1999).
 - [2] S. Datta, *Electronic Transport in Mesoscopic Systems*, Cambridge Studies in Semiconductor Physics and Microelectronic Engineering (Cambridge University Press, Cambridge, 1995).
 - [3] M. Dresselhaus, G. Chen, M. Tang, R. Yang, H. Lee, D. Wang, Z. Ren, J.-P. Fleurial, and P. Gogna, *Adv. Mater.* **19**, 1043 (2007).
 - [4] G. Benenti, G. Casati, K. Saito, and R. Whitney, *Phys. Rep.* **694**, 1 (2017).
 - [5] Y. M. Blanter and Y. V. Nazarov, *Quantum Transport: Introduction to Nanoscience* (Cambridge University Press, Cambridge, 2009).
 - [6] X. Zhang and L.-D. Zhao, *J. Materiomics* **1**, 92 (2015).
 - [7] T. A. Costi and V. Zlatic, *Phys. Rev. B* **81**, 235127 (2010).
 - [8] J. Kondo, *Prog. Theor. Phys.* **32**, 37 (1964).
 - [9] R. Scheibner, H. Buhmann, D. Reuter, M. N. Kiselev, and L. W. Molenkamp, *Phys. Rev. Lett.* **95**, 176602 (2005).
 - [10] S. Jezouin, F. D. Parmentier, A. Anthore, U. Gennser, A. Cavanna, Y. Jin, and F. Pierre, *Science* **342**, 601 (2013).
 - [11] Z. Iftikhar, S. Jezouin, A. Anthore, U. Gennser, F. D. Parmentier, A. Cavanna, and F. Pierre, *Nature (London)* **526**, 233 (2015).
 - [12] S. Jezouin, Z. Iftikhar, A. Anthore, F. D. Parmentier, U. Gennser, A. Cavanna, A. Ouerghi, I. P. Levkivskyi, E. Idrisov, E. V. Sukhorukov, L. I. Glazman, and F. Pierre, *Nature (London)* **536**, 60 (2016).
 - [13] M. Ferrier, T. Arakawa, T. Hata, R. Fujiwara, R. Delagrangé, R. Weil, R. Deblock, R. Sakano, A. Oguri, and K. Kobayashi, *Nature Phys.* **12**, 230 (2016).
 - [14] A. Svilans, M. Josefsson, A. M. Burke, S. Fahlvik, C. Thelander, H. Linke, and M. Leijnse, *Phys. Rev. Lett.* **121**, 206801 (2018).
 - [15] B. Dutta, D. Majidi, A. Garcia Corral, P. A. Erdman, S. Florens, T. A. Costi, H. Courtois, and C. B. Winkelmann, *Nano Lett.* **19**, 506 (2019).
 - [16] D. B. Karki and M. N. Kiselev, *Phys. Rev. B* **96**, 121403(R) (2017).
 - [17] J. Azema, A.-M. Daré, S. Schäfer, and P. Lombardo, *Phys. Rev. B* **86**, 075303 (2012).
 - [18] D. B. Karki and M. N. Kiselev, *arXiv:1906.00724* (2019).
 - [19] P. Jarillo-Herrero, J. Kong, H. S. van der Zant, C. Dekker, L. P. Kouwenhoven, and S. D. Franceschi, *Nature (London)* **434**, 484 (2005).
 - [20] A. Makarovski, J. Liu, and G. Finkelstein, *Phys. Rev. Lett.* **99**, 066801 (2007).
 - [21] A. Makarovski, A. Zhukov, J. Liu, and G. Finkelstein, *Phys. Rev. B* **75**, 241407(R) (2007).
 - [22] M. Ferrier, T. Arakawa, T. Hata, R. Fujiwara, R. Delagrangé, R. Deblock, Y. Teratani, R. Sakano, A. Oguri, and K. Kobayashi, *Phys. Rev. Lett.* **118**, 196803 (2017).
 - [23] T. Hata, R. Delagrangé, T. Arakawa, S. Lee, R. Deblock, H. Bouchiat, K. Kobayashi, and M. Ferrier, *Phys. Rev. Lett.* **121**, 247703 (2018).
 - [24] A. J. Keller, S. Amasha, I. Weymann, C. P. Moca, I. G. Rau, J. A. Katine, H. Shtrikman, G. Zaránd, and D. Goldhaber-Gordon, *Nature Phys.* **10**, 145 (2014).
 - [25] G. C. Tettamanzi, J. Verduijn, G. P. Lansbergen, M. Blaauboer, M. J. Calderón, R. Aguado, and S. Rogge, *Phys. Rev. Lett.* **108**, 046803 (2012).
 - [26] K. Le Hur, P. Simon, and D. Loss, *Phys. Rev. B* **75**, 035332 (2007).
 - [27] M.-S. Choi, R. López, and R. Aguado, *Phys. Rev. Lett.* **95**, 067204 (2005).
 - [28] M. Eto, *J. Phys. Soc. Jpn.* **74**, 95 (2005).
 - [29] J. S. Lim, M.-S. Choi, M. Y. Choi, R. López, and R. Aguado, *Phys. Rev. B* **74**, 205119 (2006).
 - [30] J. S. Lim, R. López, and D. Sánchez, *New J. Phys.* **16**, 015003 (2014).
 - [31] Y. Kleeorin and Y. Meir, *Phys. Rev. B* **96**, 045118 (2017).
 - [32] A. Carmi, Y. Oreg, and M. Berkooz, *Phys. Rev. Lett.* **106**, 106401 (2011).
 - [33] R. López, T. Rejec, J. Martinek, and R. Žitko, *Phys. Rev. B* **87**, 035135 (2013).
 - [34] T. Kita, R. Sakano, T. Ohashi, and S.-I. Suga, *J. Phys. Soc. Jpn.* **77**, 094707 (2008).

- [35] I. Kuzmenko and Y. Avishai, *Phys. Rev. B* **89**, 195110 (2014).
- [36] Y. Nishida, *Phys. Rev. Lett.* **111**, 135301 (2013).
- [37] J. Bauer, C. Salomon, and E. Demler, *Phys. Rev. Lett.* **111**, 215304 (2013).
- [38] Y. Nishida, *Phys. Rev. A* **93**, 011606(R) (2016).
- [39] I. Kuzmenko, T. Kuzmenko, Y. Avishai, and G.-B. Jo, *Phys. Rev. B* **93**, 115143 (2016).
- [40] C. Mora, P. Vitushinsky, X. Leyronas, A. A. Clerk, and K. Le Hur, *Phys. Rev. B* **80**, 155322 (2009).
- [41] R. Delagrangé, J. Basset, H. Bouchiat, and R. Deblock, *Phys. Rev. B* **97**, 041412(R) (2018).
- [42] P. W. Anderson, *Phys. Rev.* **124**, 41 (1961).
- [43] H. R. Krishna-murthy, J. W. Wilkins, and K. G. Wilson, *Phys. Rev. B* **21**, 1003 (1980).
- [44] L. I. Glazman and M. E. Raikh, *Pis'ma Zh. Eksp. Teor. Fiz.* **47**, 378 (1988) [*JETP Lett.* **47**, 452 (1988)].
- [45] J. R. Schrieffer and P. A. Wolff, *Phys. Rev.* **149**, 491 (1966).
- [46] O. Parcollet, A. Georges, G. Kotliar, and A. Sengupta, *Phys. Rev. B* **58**, 3794 (1998).
- [47] C. Mora, *Phys. Rev. B* **80**, 125304 (2009).
- [48] P. Nozières, *J. Low Temp. Phys.* **17**, 31 (1974).
- [49] I. Affleck and A. W. W. Ludwig, *Phys. Rev. B* **48**, 7297 (1993).
- [50] D. L. Cox and A. Zawadowski, *Adv. Phys.* **47**, 599 (1998).
- [51] D. B. Karki, C. Mora, J. von Delft, and M. N. Kiselev, *Phys. Rev. B* **97**, 195403 (2018).
- [52] D. B. Karki and M. N. Kiselev, *Phys. Rev. B* **98**, 165443 (2018).
- [53] L. V. Keldysh, *Zh. Eksp. Teor. Fiz.* **47**, 1515 (1964) [*Sov. Phys. JETP* **20**, 1018 (1965)].
- [54] T.-S. Kim and S. Hershfield, *Phys. Rev. Lett.* **88**, 136601 (2002).
- [55] T.-S. Kim and S. Hershfield, *Phys. Rev. B* **67**, 165313 (2003).
- [56] C. W. J. Beenakker and A. A. M. Staring, *Phys. Rev. B* **46**, 9667 (1992).
- [57] V. Zlatić and R. Monnier, *Modern Theory of Thermoelectricity* (Oxford University Press, Oxford, 2014).
- [58] K. A. Matveev and A. V. Andreev, *Phys. Rev. B* **66**, 045301 (2002).
- [59] A. Carmi, Y. Oreg, M. Berkooz, and D. Goldhaber-Gordon, *Phys. Rev. B* **86**, 115129 (2012).
- [60] M. Pustilnik and L. I. Glazman, *Phys. Rev. Lett.* **87**, 216601 (2001).
- [61] M. Pustilnik and L. Glazman, *J. Phys. Condens. Matter* **16**, R513 (2004).
- [62] M. Pustilnik, L. Borda, L. I. Glazman, and J. von Delft, *Phys. Rev. B* **69**, 115316 (2004).
- [63] J. Park, S.-S. B. Lee, Y. Oreg, and H.-S. Sim, *Phys. Rev. Lett.* **110**, 246603 (2013).
- [64] A. Dorda, M. Ganahl, S. Andergassen, W. von der Linden, and E. Arrigoni, *Phys. Rev. B* **94**, 245125 (2016).
- [65] D. Pérez Daroca, P. Roura-Bas, and A. A. Aligia, *Phys. Rev. B* **97**, 165433 (2018).
- [66] U. Eckern and K. I. Wysokiński, *arXiv:1904.05064* (2019).